Original Article

http://www.jcpjournal.org
pISSN 2288-3649 · eISSN 2288-3657
https://doi.org/10.15430/JCP.2023.28.4.160

JCP

Potent Suppression of Prostate Cancer Cell Growth and Eradication of Cancer Stem Cells by CD44-targeted Nanoliposome-quercetin Nanoparticles

Kader Turkekul, Suat Erdogan

Department of Medical Biology, School of Medicine, Trakya University, Balkan Campus, Edirne, Turkey

The bioavailability of quercetin, a natural compound, is hindered by low solubility, limited absorption, and restricted systemic availability. Therefore, encapsulating it in biocompatible nanoparticles presents a promising solution. This study aimed to target prostate cancer stem cells (CSCs) overexpressing CD44+ receptors as well as cancer cells, employing quercetin-loaded hyaluronic acid-modified nanoliposomes (LP-Quer-HA). Synthesized via a green ethanol injection method, these nanoliposomes had an average diameter of 134 nm and an impressive loading efficiency of 96.9%. Human prostate cancer cells were treated with either 10 μM of free quercetin or the same concentration delivered by LP-Quer-HA for 72 hours. Free quercetin reduced androgen-resistant PC3 cell viability by 16%, while LP-Quer-HA significantly increased cell death to 60%. It induced apoptosis, upregulating cytochrome *c*, Bax, caspases 3 and 8, and downregulating survivin and Bcl-2 expression. Compared to free quercetin, LP-Quer-HA upregulated E-cadherin expression while inhibiting cell migration and reducing the expression of fibronectin, N-cadherin, and MMP9. Treatment of PC3 cell tumor spheroids with LP-Quer-HA decreased the number of CD44 cells and expression of CD44, Oct3/4 and Wnt. Moreover, LP-Quer-HA inhibited p-ERK expression while increasing p38/MAPK and NF-κB protein expression. In androgen-sensitive LNCaP cells, LP-Quer-HA efficacy was notable, reducing cell viability from 10% to 52% compared to free quercetin. Utilizing HA-modified nanoliposomes as a quercetin delivery system enhanced its potency at lower concentrations, reducing the CD44+ cell population and effectively impeding prostate cancer cell proliferation and migration. These findings underscore the potential of quercetin-loaded cationic nanoliposomes as a robust therapeutic approach.

Key Words Quercetin, Liposomes, Nanoparticles, Neoplasms, Prostate cancer, Therapeutic use

INTRODUCTION

Prostate cancer is a leading global cancer among men, ranking second in diagnoses and fifth in cancer-related deaths worldwide. In 2020, there were 1,414,259 new cases, resulting in 375,304 deaths [1]. Most cases and fatalities occur in men aged 65 and older [2]. Treating prostate tumors poses significant challenges due to their multifocal nature, complexity, resistance to therapies, and tendency to metastasize to the bone in advanced stages. Treatment options include radiation therapy, immunotherapy, chemotherapy, and combinations [3]. However, these therapies have limitations such as side effects and inadequate distribution of active components. Docetaxel, a common chemotherapy agent, is effective but combining treatments is essential to overcome limitations and improve safety [4].

Tumors harbor various cell populations, including cancer stem cells (CSCs) with tumor-initiating abilities [5]. CSCs, often < 1% of tumor tissue, resist standard therapies and develop multidrug resistance [6]. They express pluripotent factors like Nanog, Oct, and Sox, and generate three-dimensional cultures [7,8]. CSCs are identified in prostate and other cancers using surface markers like CD24, CD44, and CD133 [9] [10]. CD44, pivotal in cellular functions and highly expressed in tumors, influences self-renewal, cellular environment preparation, and apoptosis resistance [11,12]. Cells expressing CD44 are notably linked to aggressive cancer phases, especially in prostate CSCs [13,14].

In normal tissues, the CD44 receptor is expressed at low levels and necessitates activation. CD44's high affinity for

Received September 22, 2023, Revised November 24, 2023, Accepted November 28, 2023
Correspondence to Suat Erdogan, E-mail: suaterdogan@trakya.edu.tr, https://orcid.org/0000-0002-6823-6293

hyaluronic acid (HA) in tumor stem cells negates its activation requirement [15], making it an ideal target for cancer therapy [16]. Surface-modified nanodrug systems with HA significantly improve targeting precision and prolong circulation, benefiting therapeutic applications [17]. Nanoliposomes ensure efficient drug delivery, solubility enhancement, and minimize side effects [18]. These delivery systems enhance the solubility of both hydrophilic and amphiphilic drugs while offering localized and sustained drug release. Flavonoids like quercetin, apigenin, and naringin are natural occurring polyphenolic compounds found in a variety of fruits and vegetables exhibit antioxidant and anti-tumor properties [19,20]. Quercetin (3,3',4',5,7-pentahydroxyflavone) is commonly found in apple, tea, strawberry, grape and onion peels. It influences cancer cells by inhibiting proliferation, arresting the cell cycle, prompting apoptosis, and modulating various pathways [21,22]. However, its limitations include chemical instability, short half-life, and poor water solubility [23]. Encapsulation within nanoparticles presents a strategy to enhance its delivery and effectiveness.

Research on quercetin nanoformulations for prostate cancer is limited. Advances in nanomicelle development have notably improved its solubility, especially for treating castration-resistant prostate cancer. *In vitro* studies show a tenfold reduction in IC_{50} compared to free quercetin, with increased apoptotic and anti-proliferative effects [24]. *In vivo* studies indicate enhanced accumulation of quercetin nanoformulations in tumors, suppressing proliferation. Targeted nanoformulations with docetaxel also exhibit higher cytotoxicity in PC3 and LNCaP cells [25]. This suggests potential efficacy in cancer treatment compared to traditional methods. Further research is needed to validate CSC-targeted quercetin efficacy. This study aims to demonstrate the effectiveness of HA-modified quercetin-loaded nanoliposomes targeting CD44+ CSCs in treating prostate cancer.

MATERIALS AND METHODS

Preparation of quercetin-loaded HA-decorated nanoliposomes

The monolayer nanoliposome formulation was created using the ethanol injection technique [26]. Initially, stock solutions of 10 mg/mL cholesterol (Sigma Aldrich), 1,2-Dioleoyl-3-dimethylammonium-propane (DOTAP; Cayman), and 2 mg/mL quercetin (Sigma Aldrich), were prepared in ethanol. Furthermore, a solution containing 1 mg/mL D-α-tocopherol polyethylene glycol succinate (TPGS) and HA was dissolved in ultrapure water. The ethanol phase containing cholesterol, DOTAP and quercetin was gradually introduced into the TPGS solution (water phase) while being stirred with a magnetic stirrer at 50ºC and 1,250 rpm until the solvent evaporated. Ultimately, the resulting nanoliposomes, suspended in ultrapure water, underwent centrifuged at 5,000 rpm for 10 minutes using ultrafiltration tubes (Merck). To identify the formulation with maximum loading efficiency, the total lipid concentration remained fixed at 0.8 mg/mL, while the quercetin/lipid ratio was maintained at 10% by weight. Various nanoliposome formulations were prepared, altering the phase volume ratios of ethanol to water (1:2.5, 1:5, and 1:10). Among these formulations, the nanoliposome suspension exhibiting the highest loading efficiency was selected. This chosen suspension was combined with an HA solution at a 1:1 ratio and incubated at room temperature. Subsequently, the resulting decorated nanoliposomes underwent centrifuged at 5,000 rpm for 10 minutes, were resuspended in ultrapure water, and then stored at +4ºC.

Size, polydispersity index and zeta potential measurements

The nanoliposomes' mean size, polydispersity index and zeta potential were determined using the laser light scattering method via a Zeta-Sizer NanoS instrument (Malvern). The nanoliposome samples were diluted tenfold with ultrapure water, and measurements were carried out in triplicate at detection angle of 1,738 degrees.

Scanning electron microscopy imaging

The structural characteristics and distribution of the nanoliposome formulations were investigated utilizing scanning electron microscopy (JEOL JCM5000). To prepare for imaging, the formulations were dropped onto aluminum plates and left to dry at room temperature before being subjected to visualization.

Nuclear magnetic resonance spectroscopy

The structural characterization of the HA-decorated nanoliposome formulation was conducted employing proton nuclear magnetic resonance spectroscopy (HNMR). Hyaluronic acid and HA-decorated nanoliposomes were dissolved in deuterium dioxide (Sigma Aldrich) and pipetted into NMR sample tubes. Spectral data were collected using a HNMR (Bruker) operating at a frequency of 500 MHz, and the chemical shift was determined in parts per million (ppm).

Quantification of quercetin

The loading efficiency assessment of the liposomal formulation was conducted using liquid chromatography-mass spectrometry/mass spectrometry. Mass spectrum measurements of quercetin within HA-modified and non-HA-modified nanoliposomes were acquired employing a 15 cm carbon-filled column featuring a pore diameter of 3.5 μm.

Cell culture

The human androgen-resistant PC3 and androgen-sensitive prostate cancer LNCaP cells, along with the normal human retinal pigment epithelial cell line ARPE-19, were obtained from the American Type Culture Collection. These cells were cultured in Dulbecco's modification of Eagle's

medium (F12), supplemented with 10% fetal bovine serum and 1% antibiotics (100 μg/mL penicillin and 100 μg/mL streptomycin; Gibco).

Cell survival test

The cells at a seeding density of 1 x 10^4 were cultured in 96-well dishes for 16 hours. Various treatments were applied for 72 hours: undecorated nanoliposomes, HA-modified nanoliposomes, nanoliposomes with 10 μM quercetin, HA-modified nanoliposomes with 10 μM quercetin, or 10 μM quercetin alone. Controls received an equivalent vehicle concentration. Afterward, fresh medium and 50 μL of MTT solution were added. Following 3 hours incubation, formazan crystals were dissolved in 200 μL of dimethyl sulfoxide (Sigma Aldrich). Absorbance at 570 nm was measured using a multi-plate reader (Multiskan GO; Thermo Scientific).

Reverse transcriptase-quantitative polymerase chain reaction

PC3 cells underwent treatment with 10 μM quercetin alone (Quer), nanoliposome containing 10 μM quercetin (LP-Quer), and HA-modified nanoliposome containing 10 μM quercetin (LP-Quer-HA) for a duration of 72 hours. Additionally, an UT received an equivalent percentage of the vehicle present in nanoliposomes. Following treatment, total RNA samples were isolated utilizing commercial kits (Bio Basic), and subsequent complementary DNA synthesis was conducted (Thermo Fisher Scientific). mRNA expression levels of selected genes were assessed using a real time polymerase chain reaction (PCR) system (Applied Biosystems).

The real-time quantitative PCR (qPCR) cycling conditions consisted of an initial denaturation for 5 minutes at 95°C, followed by 40 repeated cycles comprising 15 seconds at 95°C, 45 seconds at 60°C, and 15 seconds at 72°C. The fold enrichments of the targets were calculated using relative quantification according to the $2^{-\Delta\Delta Ct}$ method. GAPDH expression served as the internal reference gene. Each experiment was conducted with triplicate samples and repeated twice using different RNA samples. The primer pairs utilized for the amplifications were obtained from PZR Biotech and are presented in Table 1.

Wound healing assay

PC3 cells were seeded in T25 culture dishes at approximately 90% density. A wound gap was created at the base of the culture along the midline a 200 μL pipette tip. Subsequently, the cells were treated with various formulations: HA-modified nanoliposome (LP-HA), nanoliposome containing 10 μM quercetin (LP-Quer), HA-modified nanoliposome containing 10 μM quercetin (LP-Quer-HA) and 10 μM quercetin alone (Quer). Treatments continued until the wound gap in the control group was closed. The distance of the wound was measured at five different points using an imaging program and compared for analysis.

Assessment of apoptosis

Apoptosis analyzes were performed 72 hours post-exposure of cells to various treatments, including LP, LP-HA, LP-Quer, LP-Quer-HA, and 10 μM Quer. Utilizing specific kits (Life Technologies), the percentage of viable, dead and apoptotic cells was determined employing an image-based cytometer (Life Technologies) [27]. Each group underwent four separate measurements, and the experiments were repeated three times.

Additionally, apoptosis in cells treated as described above was identified via Hoechst 33342 staining. Images were captured at 340 × 510 nm using a fluorescence microscope (×40) (Axio Vert A1; ZEISS).

Tumor spheroid formation

The impact of the liposomal treatment modality on the quantity of CSCs in the bulky cell population was determined by spheroid culture. Initially, 3 × 10^6 PC3 cells were seeded in agar-coated 25 cm^2 culture dishes in serum-free medium, and subsequently exposed to LP, LP-HA, LP-Quer-HA, and Quer for 10 days. The morphological changes of the spheroid structures formed after the treatments were observed, and their images were captured using an inverted microscope.

Western blot analysis

PC3 cells were subjected to the treatment protocol outlined in the previous section, and followed by extraction of homogenates using RIPA lysis buffer (Santa Cruz Biotechnology Inc.) supplemented with protease inhibitors. Briefly, the denatured samples were loaded into 10% bis-tris gel cassettes at 50 μg/well. Post-electrophoresis, the proteins were transferred to polyvinylidene difluoride membrane (Life Technologies) using the iBlot system (Invitrogen). Subsequently, the blocked membranes were treated with cytochrome *c*, Bcl-2, p38 MAPK, NF-κB, phospho-ERK, E-cadherin, N-cadherin, matrix metalloproteinase-9 (MMP-9), fibronectin, Wnt, and β-actin primary antibodies (Novus Biologicals). This incubation occurred overnight at 4°C. Following this, the membranes were treated with appropriate IgG-containing chemiluminescence Western blot kit (Thermo Fisher Scientific). Protein bands were then analyzed using an imaging system (Bio-Rad ChemiDoc MP System).

CD44+ cell isolation

Following exposure, of PC3 cells to 10 μM quercetin (Quer) and LP-Quer-HA for 72 hours, the isolation of CD44+ stem cells was conducted utilizing a magnetic column separation system (MACS), employing a CD44 surface receptor-specific antibody (Miltenyi Biotec) as previously described [28]. Briefly, 10 × 10^6 treated cells were incubated with 100 μL of MACS buffer along with 10 μL of PE CD44 human antibody (Miltenyi Biotec). After centrifugation, the resulting pellet was resuspended in MACS buffer, and anti-PE CD44 microbeads were introduced, followed by incubation at +4°C. The su-

Table 1. Primer sequences used in PCR analyzes

Target	Forward primer sequence (5′-3')	Reverse primer sequence (5′-3')
Bax	TTGCTTCAGGGTTTCATCCA	CAGCCTTGAGCACCAGTTTG
Apaf	TGGTCAACTGCAAGGACCAT	CACGTTCAAAGGTGGCTGAT
Caspase 3	GGCATTGAGACAGACAGTGG	CATGGAATCTGTTTCTTTGC
Caspase 8	CTGCTGGGGATGGCCACTGTG	TCGCCTCGAGGACATCGCTCTC
Bax	TTGCTTCAGGGTTTCATCCA	CAGCCTTGAGCACCAGTTTG
Survivin	GACGACCCCATAGAGGAACA	GACAGAAAGGAAAGCGCAAC
CD44	TCCCAGACGAAGACAGTCCCTGGAT	CACTGGGGTGGAATGTGTCTTGGTC
Oct3/4	ACATGTGTAAGCTGCGGCC	GTTGTGCATAGTCGCTGCTTG
GAPDH	TTGGTATCGTGGAAGGACTCA	TGTCATCATATTTGGCAGGTTT

pernatant was subsequently removed viacentrifugation, and remaining cell suspension was resuspended in MACS buffer. This suspension was then loaded onto the column within a magnetic field, allowing for the elution of CD44+ stem cells within the population. Isolated CD44+ CSCs were counted under a microscope subsequent to staining with trypan blue.

Statistical analysis

The statistical analysis was conducted using SPSS v20 (IBM Corp.). Differences among numerical data were compared through one-way ANOVA, followed by Duncan's multiple range tests for multiple comparisons. Additionally, the cytotoxic IC_{50} doses of nanostructures on cells were calculated employing GraphPad Prism 7.0 software (GraphPad). Statistically significance was attributed to results with a *P*-value below 0.05.

Ethical approval

This article does not contain any studies with human participants or live animals performed by any of the authors.

RESULTS

The physicochemical characteristics of nanoliposomes

The liposomal nanoformulations were prepared using DOTAP, cholesterol, quercetin or HA in the ethanol phase. Electron microscopy revealed that the liposomal formulations displayed a spherical morphology and exhibited a nano-sized structure (Fig. 1A). To assess the antiproliferative effects of these liposomal (LP) structures, concentrations of 5 μM, 10 μM and 20 μM of free quercetin (Quer), quercetin-loaded nanoliposomes (LP-Quer) or quercetin-loaded nanoliposomes with HA (LP-Quer-HA) and their vehicles were administrated to PC3 cells for a duration of 72 hours. Then, concentration-dependent cell viability values were determined by MTT assay (Fig. 1B). Quercetin as well as its liposomal formulations, exhibited a significantly concentration-dependent inhibition of cell viability. While 10 μM quercetin applied to the PC3 cells caused 18.76% cell death, LP-Quer containing the same amount of quercetin reduced 47.79% and its vehicle LP by 19.47%. LP-Quer-HA and its vehicle LP-HA induced inhibition rates of 60.76% and 26.99%, respectively. However, concentrations below 10 μM and above (20 μM) demonstrated varying rates of cell viability inhibition, dependent on the concentration (Fig. 1B). The IC_{50} values, representing the concentration causing 50% inhibition, were as 37.1 μM for Quer, 5.48 μM for LP-Quer, and 3.77 μM for LP-Quer-HA. To assess the anti-proliferative effects of liposomal structures, 10 μM Quer and the same concentration of LP-Quer-HA or LP-Quer were administrated to PC3, LNCaP, and retinal pigment epithelial cells over a 72 hours period. Subsequently, the cytotoxic impacts of the nanoliposomes were evaluated by using MTT test. The empty LP used as vehicle decreased the survival rate of androgen-insensitive PC3 cells by 25.4% compared to the UT (Fig. 1C). Upon incorporating HA into LP (LP-HA), the reduction in viability escalated to 32.3%. The LP-Quer, the quercetin-loaded nanoliposome, induced a 46.1% decrease in cell viability. Notably, the HA-decorated quercetin-loaded nanoliposome (LP-Quer-HA) remarkably eliminated 60.1% of the cells, while. Treatment with 10 μM quercetin resulted in a mere 16.0% survival rate (Fig. 1C). In androgen-sensitive prostate cancer LNCaP cells, LP administration led to a 24.2% reduction in survival, whereas this rate increased to 29.1% in the LP-HA treated group (Fig. 1D). The use of LP-Quer caused a 49.55% reduction in cell vitality, but the most significant loss in survival was observed in the LP-Quer-HA group, with a 52.0% decrease. Treatment with nanoliposome-free quercetin (Quer) resulted in the death of only 10% of cells (Fig. 1D). The cytotoxic effect of nanoliposomes on non-cancerous cells was evaluated following a similar protocol as in previous evaluations. In retina pigment epithelial cells (ARPE-19), the administration of LP and LP-HA resulted a 3% and 1% reduction in survival, respectively, compared to the control group (Fig. 1E). LP-Quer and LP-Quer-HA demonstrated decreased cell viability by 14% and 20%, respectively. Additionally, Quer induced approximately 9% cell death in these cells (Fig. 1E). Morphological changes following nanoliposome treatment were determined under the microscope. PC3 cells were subjected to 10 μM quercetin, LP-Quer and LP-Quer-HA for 72 hours (Fig. 1F). The observed changes in morphology and cell density in culture

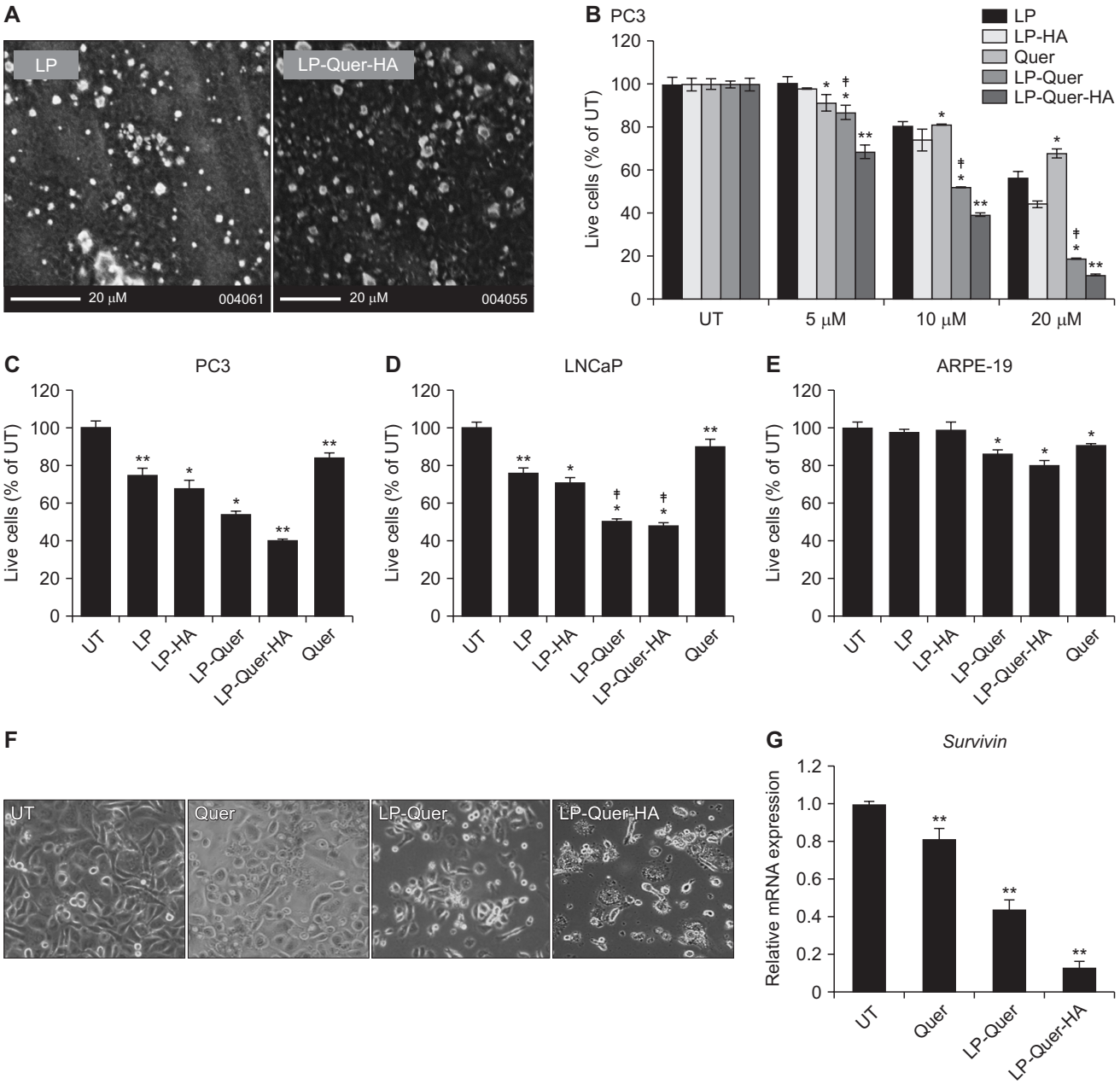

Figure 1. The physicochemical characteristics of nanoliposomes. (A) Scanning electron microscope image of liposomal formulations. (B) Dose-dependent cell viability of PC3 cells 72 hours, incubation performed in the equivalent concentration of Quer loaded HA-modified nanoliposomes. (C) 10 μM Quer and liposomal Quer formulations treated PC3, (D) LNCaP cells, and (E) ARPE-19 cell viability. (F) Microscopic visualization of PC3 cells, 10 μm Quer, liposomal Quer, and HA-modified Quer loaded nanoliposomes after 72 hours incubation period. (G) Relative survivin mRNA expression levels were determined by RT-qPCR in PC3 cells. Target gene expressions were normalized to that of GAPDH. UT, untreated; LP, nanoliposomes; LP-HA, hyaluronic acid-modified nanoliposomes; Quer, quercetin; LP-Quer, quercetin-loaded nanoliposomes; LP-Quer-HA, hyaluronic acid-modified, quercetin-loaded nanoliposomes. *P < 0.05 vs. UT, **P < 0.001 vs. all groups, ‡P < 0.05 vs. LP-HA.

post-treatment correlated with the data indicating cell viability inhibition.

The mRNA expression level of the survivin gene, commonly linked to apoptosis inhibition and decreased cell death in tumors was examined using real-time RT-qPCR. The finding showed that Quer, LP-Quer and LP-Quer-HA led to a down-regulation in Survivin mRNA expression by 19%, 57%, and 87%, respectively, when compared to untreated cells (Fig. 1G).

Loading efficiency

The loading efficiency assessment revealed that LP-Quer

had a loading efficiency of 95.13%, whereas LP-Quer-HA exhibited a loading efficiency of 96.91% as determined through chromatographic analysis.

Size and zeta potential

The nanoformulations displayed an average size consistently below than 150 nm (Fig. 2A) with polydispersity indices below 0.3 (Table 2). Regarding zeta potentials, the HA-modified

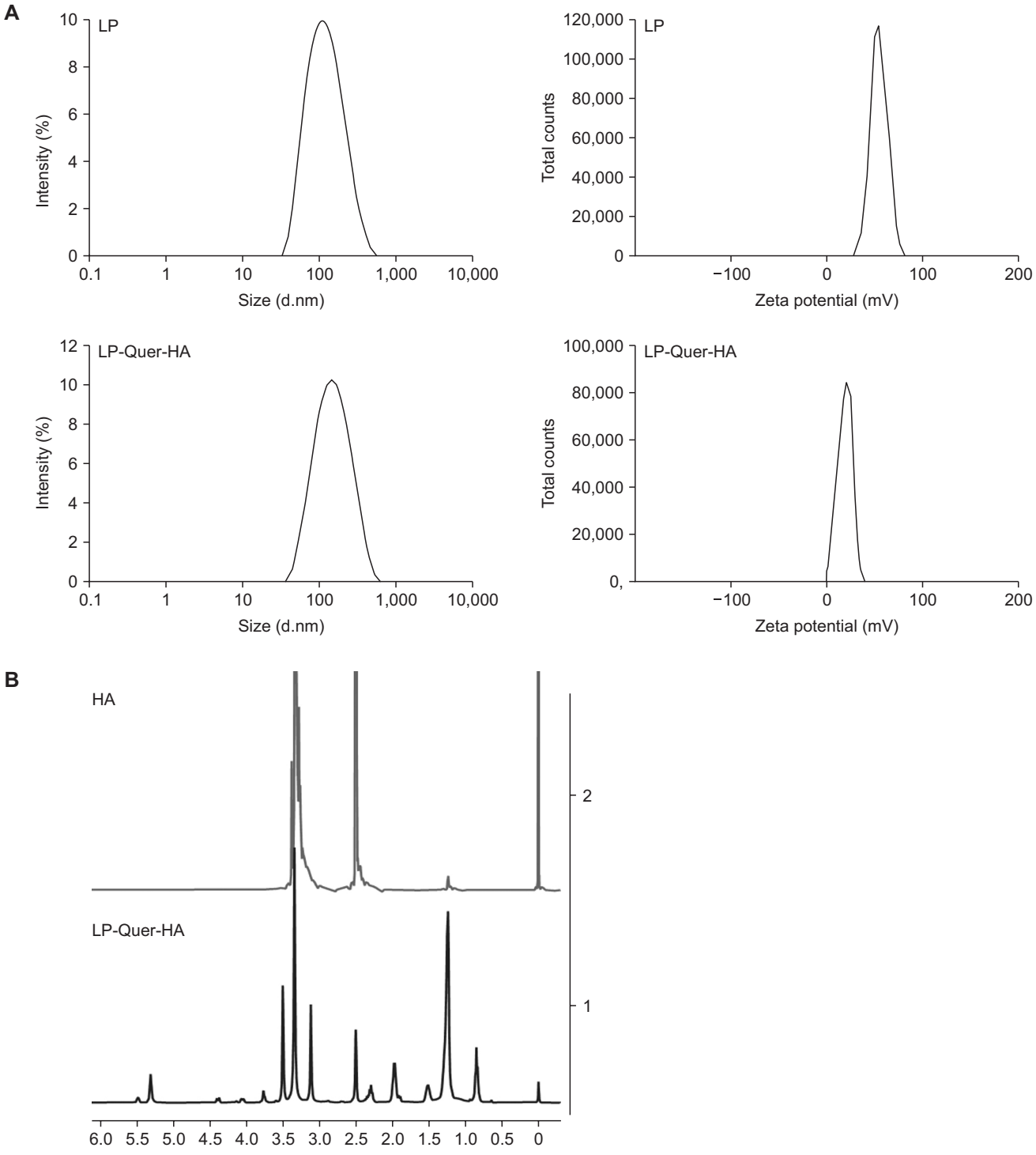

Figure 2. The characterization of liposomal formulations. Size distribution and zeta potential (A) plots of liposomal formulations. (B) NMR spectra of HA and formulation of LP-Quer-HA. NMR, nuclear magnetic resonance spectroscopy; LP, nanoliposome; LP-Quer-HA, hyaluronic acid-modified, quercetin-loaded nanoliposomes.

Table 2. Physicochemical characteristics of nanoliposomes before and after modification of hyaluronic acid

	Size (nm)	Zeta potential (mV)	PDI
LP	107.9 ± 2.51	50.24 ± 0.17	0.17 ± 0.01
LP-HA	129.6 ± 3.21	4.62 ± 0.37	0.240 ± 0.12
LP-Quer	118.3 ± 4.58	59.1 ± 0.70	0.279 ± 0.10
LP-Quer-HA	134.6 ± 6.08	18.8 ± 0.53	0.293 ± 0.16

Each run was done in triplicate and data was represented as mean ± standard deviation. PDI, polydispersity indices; LP, nanoliposomes; LP-HA, hyaluronic acid-modified nanoliposomes; LP-Quer, quercetin-loaded nanoliposomes; LP-Quer-HA, hyaluronic acid-modified, quercetin-loaded nanoliposomes.

liposomal formulations exhibited notably reduced values in comparison to the HA-free LP and LP-Quer variants (Table 2). The decline in charge of the unmodified nanoliposomal formulation from 50.24 mV to 4.62 mV indicates a significant alteration in the liposomal surface due to the modification process.

Nuclear magnetic resonance

The methyl groups in the N-acetyl functional group in the HA skeleton showed a chemical shift at 2.1 ppm. Anomeric protons in the hyaluronic skeleton were observed in the range of 3.2 to 3.5 ppm band. Additionally, new peaks were identified at 0.85 ppm corresponding to methyl groups and at 1.26 ppm ppm corresponding to methylene groups within the lipid chain (Fig. 2B).

Nanoliposomal quercetin induces apoptosis

The apoptotic effects of either 10 μM quercetin or liposomal formulations with an equal concentration were assessed in PC3 cells following 72 hours treatment. Among the liposomal administrations, the highest apoptotic activity in liposomal administrations was observed in LP-Quer-HA with 24%, surpassing the 11% observed in the Quer treatment group (Fig. 3A). LP-Quer induced apoptosis at a rate similar to Quer. However, neither LP nor LP-HA induced apoptosis (Fig. 3A). Non-apoptotic cell death was occurred at rates 11.6%, 26.3%, and 23.6% in the LP, LP-HA and LP-Quer treated cells, respectively, while it was 49.3% in LP-Quer-HA treatment (Fig. 3A). In Quer application, there was no significant difference compared to untreated cells. Hoechst 33342 staining illustrated a high presence of apoptosis in LP-Quer-HA cells, showcasing apoptotic bodies and chromatin condensation (Fig. 3C).

Administration of LP-Quer-HA led to an upregulated Bax, Apaf, caspase 3 and caspase 8 mRNA expression by 1.6, 1.9, 3.1, and 4.8-fold, respectively (Fig. 3B). Cells treated with LP-Quer-HA showed the highest expression of anti-apoptotic Bcl-2 protein relative to untreated cells. Quer, LP-HA and LP-Quer significantly reduced Bcl-2 protein expression, albeit to a lesser extent compared to the untreated group (Fig. 3D). Moreover, the expression level of cytochrome *c* protein increased by 6.8-fold in LP-Quer-HA treated cells compared to untreated cells, while this increase was 3.0, 3.9, and 2.2 in LP-HA, LP-Quer and Quer treatments, respectively (Fig. 3E).

Nanoliposomes attenuate stemness properties

The cytotoxic effectiveness of CD44-targeted quercetin treatment on the CSC population was assessed through multiple methods. Initially, the quantification of CSCs post-treatment in PC3 cells was conducted. Treatment with Quer reduced the number of CD44+ stem cells by only 14.5% compared to the control group, while this reduction was significantly higher at 79.3% in cells treated with LP-Quer-HA (Fig. 4A). Additionally, morphological changes of three-dimensional spheroid structures formed by stem cells were observed based on different treatments. LP-Quer-HA-treated cells displayed limited spheroid formation, composed of fewer cells, while the untreated and vehicle-treated groups maintained larger, denser structures (Fig. 4B). Cells treated with Quer and LP-Quer formed smaller, more compact spheroids (Fig. 4B). Furthermore, the impact treatment modalities on stem cell markers were evaluated. The mRNA expression of CD44 cell surface receptor (Fig. 4C) and Oct3/4 transcription factor (Fig. 4D) in LP-Quer-HA treated cells was showed significant downregulation, reduced by 59% and 86%, respectively, compared to untreated cells. The investigation focused on of Wnt protein expression, pivotal in regulating the self-renewal and differentiation of CSCs. The findings revealed a considerable discrepancy in inhibiting Wnt protein expression levels between liposomal quercetin formulations and the non-liposomal form, Quer (Fig. 4E). Both LP-Quer and LP-Quer-HA exhibited a similar level of inhibition on Wnt expression, whereas LP-HA and Quer had a comparatively lower impact.

Quercetin in nanostructure inhibits cell migration

Whether the liposomal structures of quercetin prevent cell migration was evaluated by the wound healing assay. 10 μM Quer or its liposomal formulations administrated to PC3 cells. The experiment was terminated when the wound gap in the untreated cells was completely closed (Fig. 5A). LP-HA showed ineffectiveness, while Quer alone inhibited migration by 20% (Fig. 5B). LP-Quer-HA demonstrated a substantial 75% inhibited, whereas suppression was 50% in LP-Quer (Fig. 5A and 5B). Expression of adhesion-mediating protein E-cadherin significantly differed among treatment groups. LP-HA upregulated its expression 2.0-fold, LP-Quer by 3.8-fold, Quer by 3.5-fold, and LP-Quer-HA by 4.4-fold (Fig. 5C). N-cadherin protein expression was significantly consistently by 50% in all groups compared to the control (Fig. 5D). Fibronectin, responsible for the mesenchymal epithelial transition, was notably reduced in LP-Quer-HA and LP-Quer-treated cells, exhibiting 70% and 63% inhibition, respectively, compared to control (Fig. 5E). Expression of fibronectin in

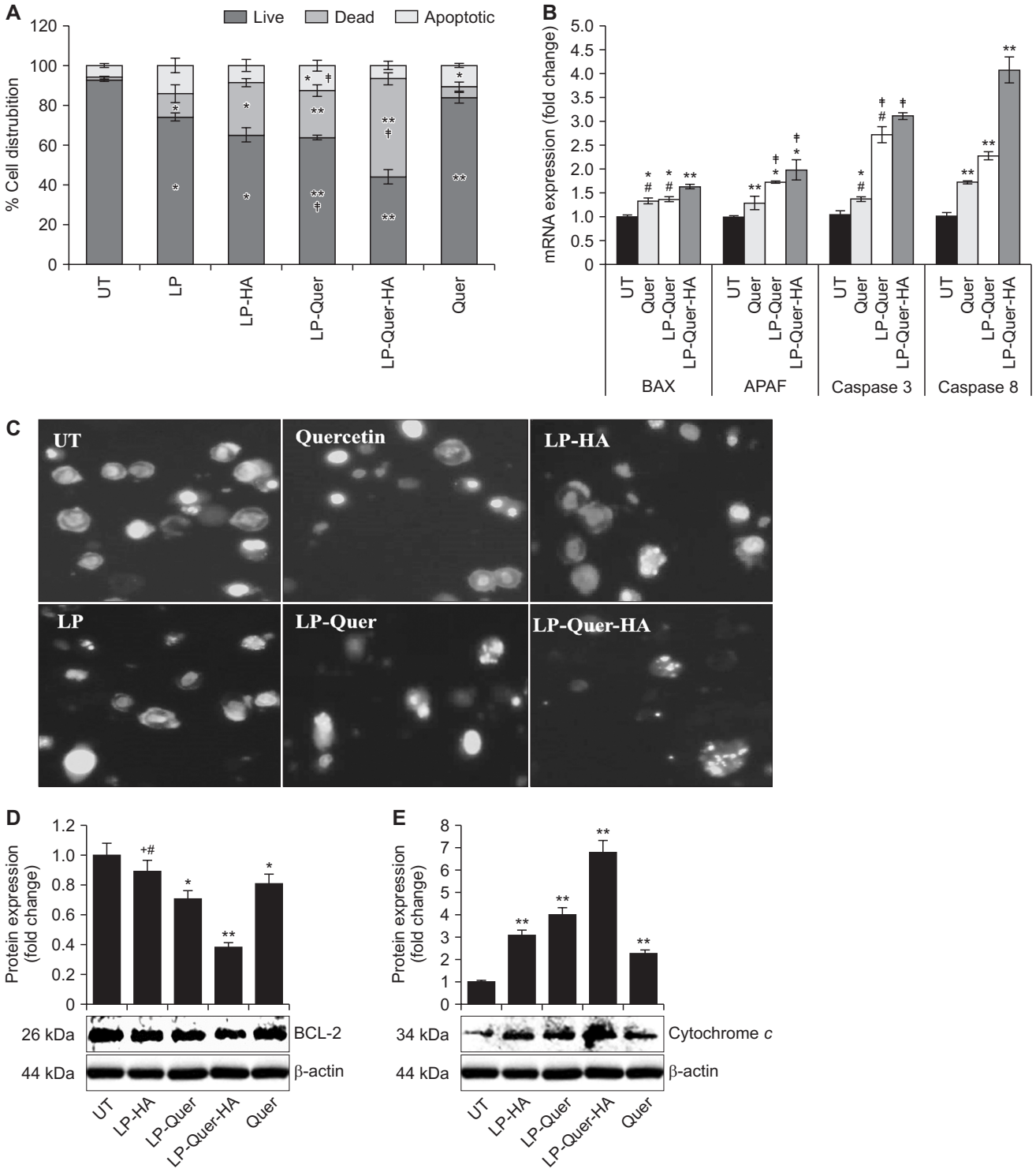

Figure 3. Apoptosis induction of liposomal treatment. (A) Live, dead and apoptotic cell distribution of PC3 cells were quantitatively assessed by annexin V/propidium iodide staining using image-based cytometer. (B) Each column represents the mean ± regulation of apoptotic genes. All data were performed in triplicate and values are means of the two different experiments ± standard deviation. Apoptotic cells detected by Hoechst staining. (C) RT-qPCR mRNA expressions of BAX, APAF, Caspase 3, Caspase 8 were analyzed 72 hours after treatment. (D) Treatment cells with liposomal Quer significantly inhibited the expression levels of antiapoptotic Bcl-2 protein, and (E) upregulated apoptotic cytochrome *c* protein. UT, untreated; LP, nanoliposomes; LP-HA, hyaluronic acid-modified nanoliposomes; Quer, quercetin; LP-Quer, quercetin-loaded nanoliposomes; LP-Quer-HA, hyaluronic acid-modified, quercetin-loaded nanoliposomes. **P* < 0.001 vs. UT, $^{\#}$*P* < 0.001 vs. LP-Quer-HA, ‡*P* < 0.001 vs. Quer, ***P* < 0.001 vs. all groups.

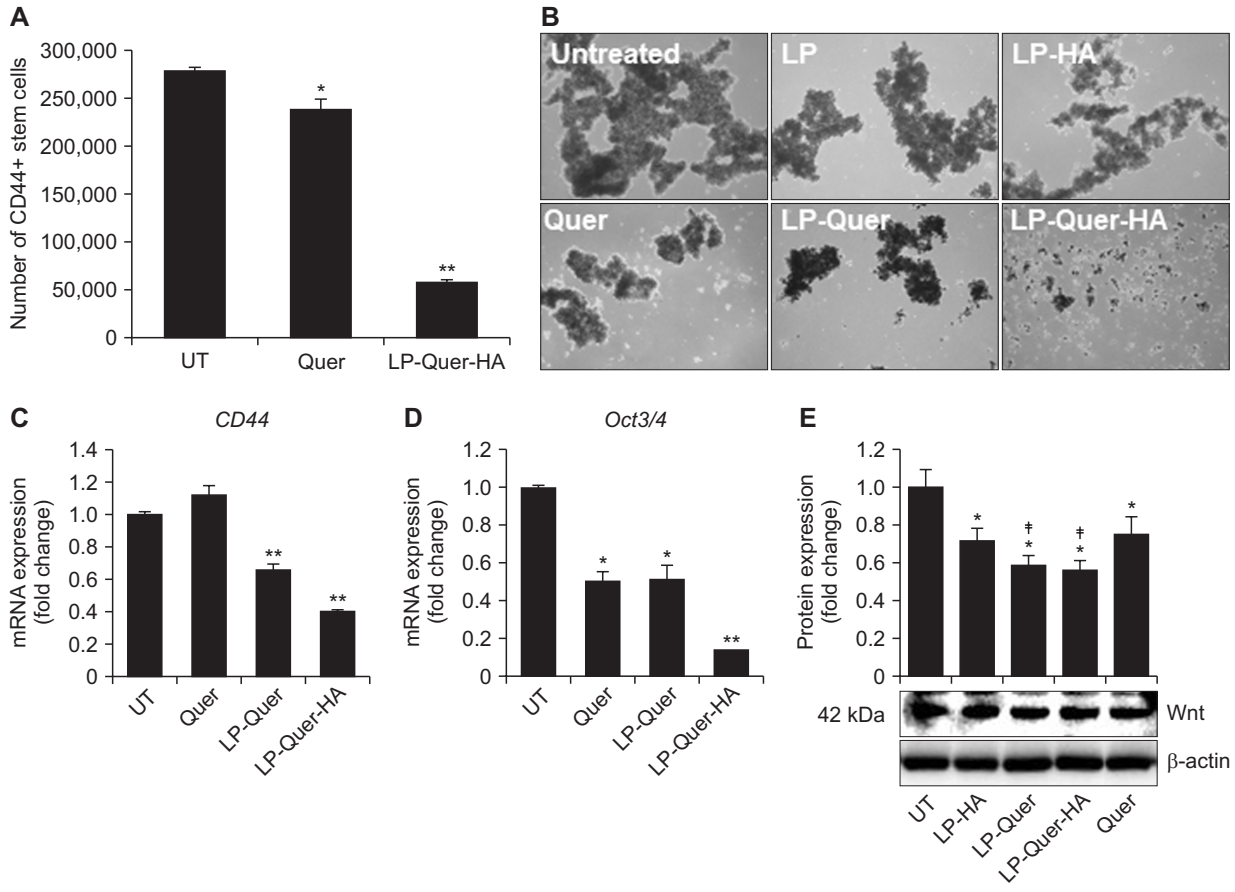

Figure 4. Hyaluronic acid-modified nanoliposomes effects on stemness properties. (A) Number of CD44+ cancer stem cells in Quer alone and HA-modified liposomal Quer treated cells were counted after magnetic separation. (B) Spheroid formation assay performed in serum-free media and captured (×10) at the end of the incubation period. (C) LP-Quer-HA suppresses CD44 and (D) Oct3/4 mRNA expression. RT-qPCR mRNA expressions were performed triplicate and GAPDH was used as housekeeping gene. Western blot results indicated that liposomal Quer treated PC3 cells shown less Wnt (E) protein expression than Quer alone. Densitometry analysis performed to quantify the results and, beta actin used as loading control. UT, untreated; LP, nanoliposomes; LP-HA, hyaluronic acid-modified nanoliposomes; Quer, quercetin; LP-Quer, quercetin-loaded nanoliposomes; LP-Quer-HA, hyaluronic acid-modified, quercetin-loaded nanoliposomes. *P < 0.001 vs. UT, **P < 0.001 vs. all groups, ‡P < 0.05 vs. LP-HA.

Quer and LP-HA cells was inhibited by 58% and 26%, respectively, compared to untreated cells (Fig. 5E). MMP-9 protein expression was significantly inhibited by Quer, LP-Quer-HA, LP-Quer, and LP-HA by 18%, 62%, 47%, and 25%, respectively, compared to the untreated cells. The highest inhibition was observed in LP-Quer and LP-Quer-HA treatments (Fig. 5F).

Nanoliposomal formulations alter protein expression

Alterations in the protein expression of p38 MAPK and p-ERK were assessed in PC3 cells upon exposure to nanoliposomes carrying 10 μM quercetin. Quer elevated p38 MAPK expression by 2.34-fold in compared to untreated cells. LP-Quer and LP-Quer-HA formulations demonstrated increased upregulation by 5.09 and 4.99-fold changes, respectively (Fig. 6A). Conversely, LP-HA exhibited no discernible impact on p38 MAPK expression. The expression of p-ERK was notably downregulated by Quer, LP-Quer and LP-Quer-HA formulations when compared to untreated cells, whereas LP-HA demonstrated no effect (Fig. 6B). Furthermore, both Quer and its lysosomal formulations exhibited a significant increase in the protein expression of NF-κB p105 (Fig. 6C) and p50 (Fig. 6D) subunits in contrast to untreated cells.

DISCUSSION

Natural substances like flavonoids hold promise against cancer, but their effectiveness as drugs is limited by issues like poor solubility, limited absorption, and quick metabolism [28,29], hindering their medical utility. Drug delivery systems enhance solubility and ensure precise delivery to target tissues [30]. Nano-formulations of flavonoids like quercetin, curcumin, and apigenin show promise in cancer prevention or treatment [21,31]. However, quercetin faces challenges in pharmaceutical use due to poor solubility, delivery limitations,

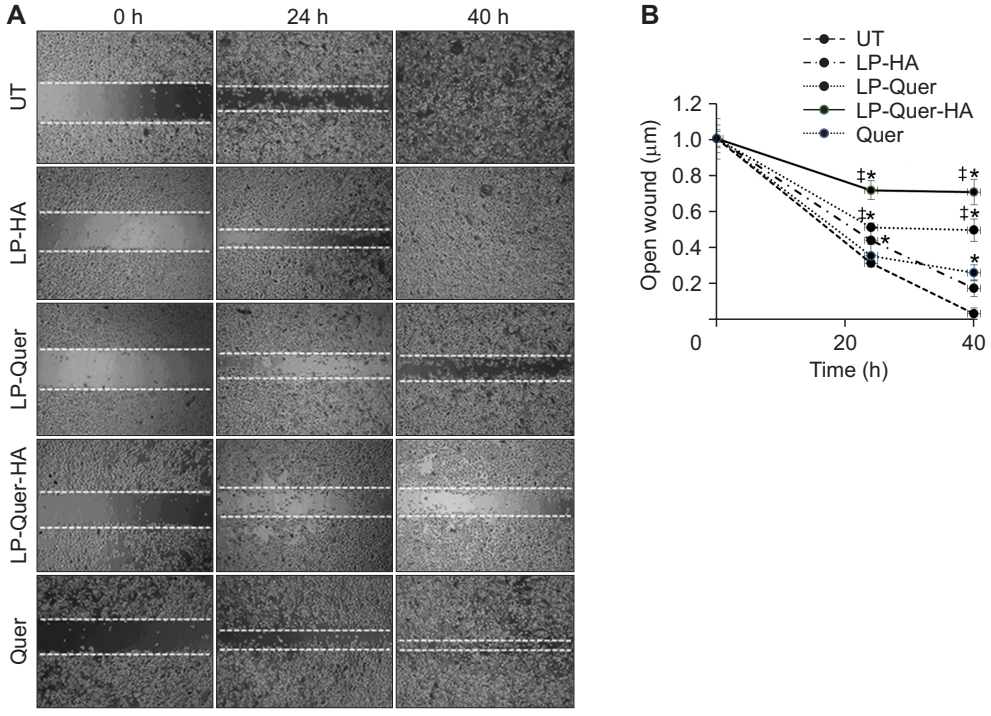

Figure 5. Effect of liposomal Quer on cell migration and protein expression. PC3 cell migration was determined by wound healing assay during 30 hours treatment in serum-free medium. (A) Hyaluronic acid-modified and non-modified liposomal Quer inhibited cell migration (×10). (B) The migration ratio (%) was calculated by measuring the wound gaps. Protein lysates were analyzed by Western blotting. Beta-actin was used as loading control. (C) Protein expression E-Cadherin, (D) N-Cadherin, (E) fibronectin, and (F) MMP-9 given as fold changes of each protein compared to loading control. The intensities of immunoreactive bands were quantified by densitometric analysis. UT, untreated; LP, nanoliposomes; LP-HA, hyaluronic acid-modified nanoliposomes; Quer, quercetin; LP-Quer, quercetin-loaded nanoliposomes; LP-Quer-HA, hyaluronic acid-modified, quercetin-loaded nanoliposomes. *$P < 0.01$ vs. UT, **$P < 0.001$ vs. all groups, $^{‡}P < 0.05$ vs. Quer.

and low bioavailability. Despite ongoing research, practical applications of quercetin-loaded delivery systems remain unrealized. There's also a gap in using nanoparticles with quercetin to target CSCs. This study seeks to boost quercetin's therapeutic effectiveness and precision in targeting CSCs through specialized nanoliposome formulation.

The favorable physicochemical properties of LP-Quer-HA were validated through SEM analysis and measurements of mean particle size, zeta potential, and loading efficiency. The prepared NL-Quer-HA formulations showcased notable enhancements compared to prior reports on quercetin-loaded nanoliposomes [23,32]. Treatment involving liposomal quercetin exhibited a dose-dependent cytotoxic effect on PC3 cells, resulting in a significant reduction in cell viability. The liposomal formulation decreased the IC_{50} value by 6.7-fold, while the HA-modified liposomal quercetin further reduced it by 9.8-fold. Previous studies reported a 90% decrease in the IC_{50} value of micellar quercetin in castration-resistant prostate cancer cells [24] and an 83.8% decrease in the IC_{50} value of hydrogel nanoformulated quercetin in hormone-sensitive breast cancer cells [33]. Given the expression of CD44s and CD44v proteins in prostate cancer PC3 and LNCaP cell lines [34], it was anticipated that HA-modified nanoliposomal formulations would exhibit similar cytotoxic effects in both androgen-sensitive and androgen-insensitive cells. However, this study observed, 9.7% higher cytotoxicity of nanoliposomal quercetin in LNCaP cells compared to PC3 cells. Earlier data suggested that PC3 cells are more sensitive to cationic liposomes [35], but other components within the liposomal formulation might have heightened the sensitivity of LNCaP cells. Specifically, TPGS induced DNA damage in AR-positive LNCaP cells but did not evoke a similar response in AR-negative PC3 and DU145 cells [36]. In the context of prostate cancer, cabazitaxel and silibinin, encapsulated within HA-modified cationic nanoliposomes, effectively targeted CD44 receptors, inhibiting cell migration and promoting apoptosis [37]. Furthermore, a nanocarrier loaded with quercetin and docetaxel exhibited cytotoxic effects on breast cancer cells [38]. The present study emphasizes the significant enhancement of HA-modified liposomal quercetin's efficacy compared to free quercetin. Notably, the delivery system showed minimal detrimental effects on normal cells, such as retinal pigment epithelial cells, indicating its advantages.

In a prior investigation, our team provided evidence that the application of 40 μM quercetin significantly reduced cell survival in both PC3 and CD44+ cells [39]. This effect was achieved through G1 cell cycle arrest and the induction of both necrosis and apoptosis. In the present study, the decline

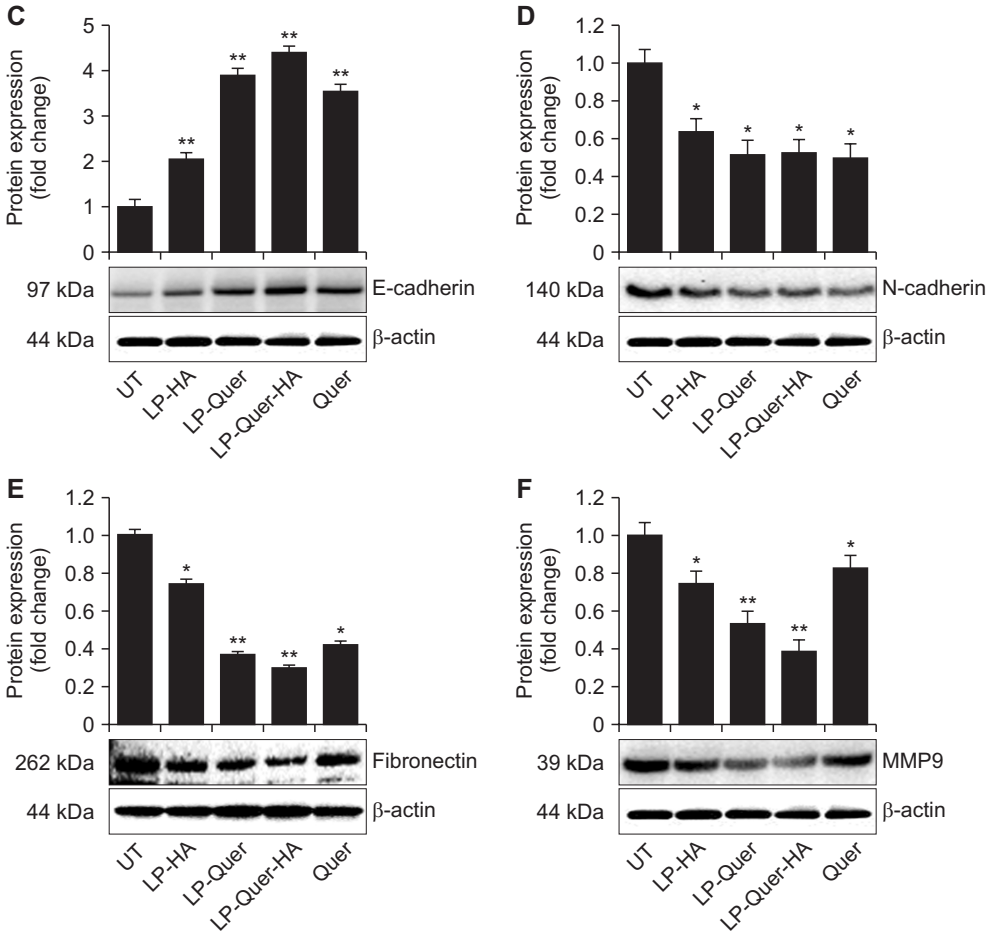

Figure 5. Continued.

in cell survival observed in PC3 cells exposed to LP-Quer-HA is attributed, at in part, to both apoptotic and non-apoptotic mechanisms of cell death. Prostate CSCs demonstrate elevated surface expression of CD44 compared to other cancer cells [40]. To specifically target CD44 receptors, anionic polysaccharide HA was utilized to coat cationic nanoliposomes. Consequently, the therapeutic effectiveness of HA-modified liposomal formulations loaded with quercetin, aiming to target CD44 surface receptors in prostate CSCs, was investigated. Quercetin has exhibited to suppress the pluripotency of CSCs in prostate [41] and pancreatic cancers [42]. In our previous studies, we demonstrated that CD44+/133+ prostate CSCs were sensitive to quercetin treatment, leading to the inhibition of the PI3K/AKT and ERK signaling pathways [39]. Moreover, quercetin has been reported to induce cell cycle arrest, apoptosis, and prevent migration in both androgen-sensitive and androgen-resistant CD44+ prostate CSCs [39]. Quercetin administration has also been found to diminish the pluripotency properties of DU145 cells by inhibiting the JNK pathway [41]. The observed 34% decrease in CD44 mRNA expression following LP-Quer treatment suggests a more efficient uptake of quercetin in liposomal form, resulting in the suppression of CSC properties. Additionally, the 60% suppression of CD44 expression in cells treated with LP-Quer-HA confirms the successful modification with HA. While free quercetin reduced the number of CD44+ stem cells by 14.4% compared to untreated cells, LP-Quer-HA reduced it by 79.3%. The decrease in the number of CD44+ CSCs within the cancer population due to free quercetin might be attributed to its suppression of stem cell properties. This could be explained by the fact that the intracellular uptake of HA-modified nanoformulations through receptor-mediated endocytosis is a more efficient transport mechanism compared to the passive diffusion of non-HA-modified nanoformulations across the cell membrane, as previously reported [43].

Nanoformulations containing curcumin, a phenolic molecule, effectively targeted CSCs, reducing their capacity for spheroid formation by suppressing Nanog, Sox and OCT3/4 protein expression in breast cancer cells and their CSCs [44]. Immunoblotting data revealed a significant inhibition of Wnt protein expression across all treatments compared to the control. RT-qPCR analyses displayed no significant difference in Oct3/4 mRNA inhibition rates between cells treated with free quercetin and nanoliposomal quercetin. However, cells

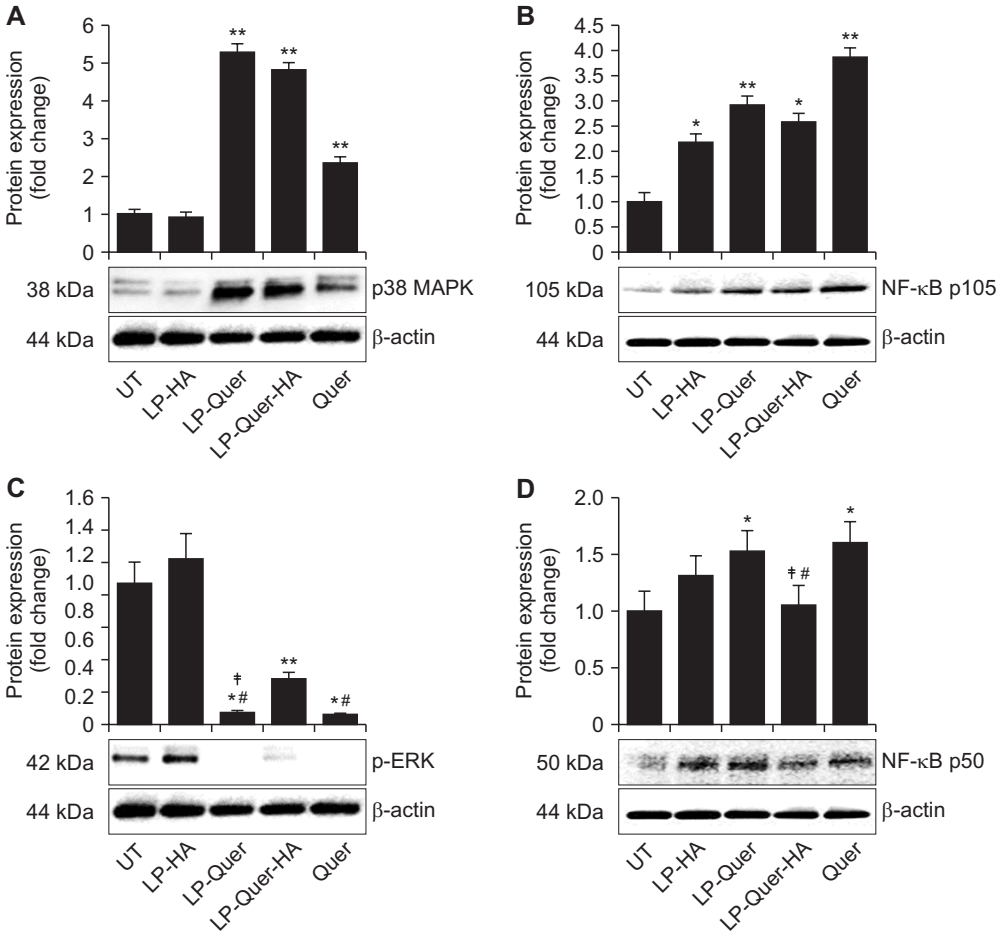

Figure 6. The effects of liposomal Quer on different signaling pathways. PC3 cells were treated with liposomal Quer, HA-modified liposomal Quer and, free Quer (10 μM) for 72 hours, isolated protein samples were then subjected to Western blotting. (A) Liposomal Quer regulates p38 MAPK, (B) p-ERK, (C) NF-κB p105, and (D) NF-κB p50. UT, untreated; LP, nanoliposomes; LP-HA, hyaluronic acid-modified nanoliposomes; Quer, quercetin; LP-Quer, quercetin-loaded nanoliposomes; LP-Quer-HA, hyaluronic acid-modified, quercetin-loaded nanoliposomes. *P < 0.001 vs. UT, #P < 0.001 vs. LP-Quer-HA, ‡P < 0.001 vs. Quer, **P < 0.001 vs. all groups.

exposed to LP-Quer-HA demonstrated an 86% decrease in Oct3/4 expression, indicating the efficacy of the stem cell-targeted treatment. CSCs within a heterogeneous tumor mass are capable of forming three-dimensional spheroids in serum-free conditions [45]. The observed limited spheroid formation capacity observed in cells exposed to liposomal formulations under serum-free conditions, particularly with LP-Quer-HA, aligns with findings by Das et al. [44].

The interaction between HA and CD44 significantly impacts tumor cell survival, angiogenesis, cell migration, and metastasis processes [46]. Despite these disadvantages, novel treatment strategies are emerging that target the CD44 surface receptor, highly expressed in CSCs, to bolster the therapeutic efficacy of drugs [17]. E-cadherin serves as a recognized tumor suppressor protein, and diminished expression in tumor cells is frequently observed during tumor progression and metastasis, often associated with EMT [47]. In tumor cells where E-cadherin expression is lost, β-catenins, essential in mediating Wnt signaling, accumulate in high levels within the cytoplasm and translocate to the cell nucleus. Once in the nucleus, they bind to members of the transcription factor/lymphoid enhancer-binding factor 1 family, thereby contributing to tumor progression by activating Wnt target genes, like CD44, c-Myc and MMP-9 [48]. In this context, the noteworthy upregulation of E-cadherin observed in cells treated with LP-Quer-HA is of significance. E-cadherin forms a complex with β-catenin, impeding preventing its translocation to the nucleus. The phenomenon supports the suppression of Wnt protein expression and its downstream target genes, such as CD44 and MMP-9, aligning well with prior reports. This suggests that the observed alterations contribute to the formation of the E-cadherin/β-catenin complex, which plays a role in modulating Wnt signaling and its associated gene expression patterns.

In contrast to E-cadherin, increased N-cadherin expression has been associated with tumor cell migration and metas-

tasis [49]. It was observed that both quercetin and nanoliposomal formulations suppressed the protein expression of N-cadherin and fibronectin across all treated cells. Martinucci et al. [50] proposed that elevated fibronectin expression levels in prostate cancer cells are associated with increased invasiveness via N-cadherin and integrins, potentially contributing to resistance against apoptosis by upregulating Bcl-2 expression while downregulating Bax expression. Drawing from this insight, it can be inferred that the suppression of fibronectin expression partially contributes to the increase in Bax mRNA levels, which are associated with apoptosis, and the decrease in Bcl-2 protein expression. To summarize, the decrease in protein levels related to mesenchymal markers and the increase in E-cadherin expression observed in cells treated with LP-Quer-HA collectively contribute to inhibiting cell migration and reducing spheroid formation capacity. Additionally, the indirect induction of apoptosis and the inhibition of cell viability through integration with cell proliferation pathways play roles in resisting cell survival. Quercetin has been shown to elevate intracellular reactive oxygen species (ROS) levels and trigger endoplasmic reticulum stress in prostate cancer, leading to cell cycle arrest at the G2/M phase [51]. The increase in p38/MAPK protein expression observed in cells exposed to LP-Quer and LP-Quer-HA aligns with our prior investigation [39] and findings from other studies [51]. These data suggest that targeted nanoliposomal quercetin treatment induces an increase in p38/MAPK expression, promoting ROS production and ultimately resulting in cancer cell death.

The overall reduced activity of the transcription factor NF-κB impacts the regulation of anti-apoptotic proteins like Bcl-2 and Bcl-xL [52,53]. Activated NF-κB in cancer cells is commonly associated with tumorigenesis, inhibiting apoptosis, promoting cell proliferation, and stimulating cell migration [53]. Quercetin treatment initially triggers NF-κB activation in PC3 cells, but extended exposure eventually leads to suppression of NF-κB activity. This suggests that quercetin treatment can stimulate NF-κB activity in a pro-apoptotic manner [29]. NF-κB, when activated, can upregulate pro-apoptotic targets while suppressing anti-apoptotic ones potentially leading to apoptosis. Additionally, NF-κB's interaction with death receptors ca-n activate caspase 8, initiating cell death [54]. The varying effects of NF-κB, whether anti-apoptotic, pro-apoptotic, or apoptotic, can depend on different cellular dynamics, the concentration of quercetin applied, and the duration of incubation [29].

In conclusion, this study suggests that nanoformulations could enhance quercetin's treatment effectiveness, notably decreasing the CSC population through considerable cell death compared to free quercetin in prostate cancer PC3 cells. Targeted therapy using nanoliposomes suppresses CSC markers and reduces their capacity to form spheroids. Furthermore, the cancer stem cell-targeted quercetin therapy displays promising potential in robustly inhibiting cell migration. These findings collectively highlight the promise of quercetin nanoliposomal formulations as a pharmacological intervention for prostate tumor treatment. Subsequent research endeavors could unveil its effective utilization in live organisms.

FUNDING

This study was funded by Scientific Research Projects Coordination Unit of Trakya University (Project number: 2017-137).

CONFLICTS OF INTEREST

No potential conflicts of interest were disclosed.

ORCID

Kader Turkekul, https://orcid.org/0000-0002-0971-9690
Suat Erdogan, https://orcid.org/0000-0002-6823-6293

REFERENCES

1. Sung H, Ferlay J, Siegel RL, Laversanne M, Soerjomataram I, Jemal A, et al. Global cancer statistics 2020: GLOBOCAN estimates of incidence and mortality worldwide for 36 cancers in 185 countries. CA Cancer J Clin 2021;71:209-49.
2. Rawla P. Epidemiology of prostate cancer. World J Oncol 2019;10:63-89.
3. Litwin MS, Tan HJ. The diagnosis and treatment of prostate cancer: a review. JAMA 2017;317:2532-42.
4. Omabe K, Paris C, Lannes F, Taïeb D, Rocchi P. Nanovectorization of prostate cancer treatment strategies: a new approach to improved outcomes. Pharmaceutics 2021;13:591.
5. Testa U, Pelosi E, Castelli G. Cancer stem cell targeted therapies. Ann Ist Super Sanita 2020;56:336-50.
6. Serttas R, Erdogan S. Pretreatment of prostate cancer cells with salinomycin and Wnt inhibitor increases the efficacy of cabazitaxel by inducing apoptosis and decreasing cancer stem cells. Med Oncol 2023;40:194.
7. Papaccio F, Paino F, Regad T, Papaccio G, Desiderio V, Tirino V. Concise review: cancer cells, cancer stem cells, and mesenchymal stem cells: influence in cancer development. Stem Cells Transl Med 2017;6:2115-25.
8. Monteiro N, Martins A, Reis RL, Neves NM. Liposomes in tissue engineering and regenerative medicine. J R Soc Interface 2014;11:20140459.
9. Maitland NJ, Collins AT. Prostate cancer stem cells: a new target for therapy. J Clin Oncol 2008;26:2862-70.
10. Huang JL, Oshi M, Endo I, Takabe K. Clinical relevance of stem cell surface markers CD133, CD24, and CD44 in colorectal cancer. Am J Cancer Res 2021;11:5141-54.
11. Pan Q, Li Q, Liu S, Ning N, Zhang X, Xu Y, et al. Concise review: targeting cancer stem cells using immunologic approaches.

Stem Cells 2015;33:2085-92.
12. Kushwaha PP, Verma S, Kumar S, Gupta S. Role of prostate cancer stem-like cells in the development of antiandrogen resistance. Cancer Drug Resist 2022;5:459-71.
13. Orian-Rousseau V. CD44, a therapeutic target for metastasising tumours. Eur J Cancer 2010;46:1271-7.
14. Chanmee T, Ontong P, Kimata K, Itano N. Key roles of hyaluronan and its CD44 receptor in the stemness and survival of cancer stem cells. Front Oncol 2015;5:180.
15. Gupta RC, Lall R, Srivastava A, Sinha A. Hyaluronic acid: molecular mechanisms and therapeutic trajectory. Front Vet Sci 2019;6:192.
16. Todaro M, Alea MP, Di Stefano AB, Cammareri P, Vermeulen L, Iovino F, et al. Colon cancer stem cells dictate tumor growth and resist cell death by production of interleukin-4. Cell Stem Cell 2007;1:389-402.
17. Wickens JM, Alsaab HO, Kesharwani P, Bhise K, Amin MCIM, Tekade RK, et al. Recent advances in hyaluronic acid-decorated nanocarriers for targeted cancer therapy. Drug Discov Today 2017;22:665-80.
18. Immordino ML, Dosio F, Cattel L. Stealth liposomes: review of the basic science, rationale, and clinical applications, existing and potential. Int J Nanomedicine 2006;1:297-315.
19. Panche AN, Diwan AD, Chandra SR. Flavonoids: an overview. J Nutr Sci 2016;5:e47.
20. Erdogan S, Doganlar O, Doganlar ZB, Serttas R, Turkekul K, Dibirdik I, et al. The flavonoid apigenin reduces prostate cancer CD44(+) stem cell survival and migration through PI3K/Akt/NF-κB signaling. Life Sci 2016;162:77-86.
21. Biswas P, Dey D, Biswas PK, Rahaman TI, Saha S, Parvez A, et al. A comprehensive analysis and anti-cancer activities of quercetin in ROS-mediated cancer and cancer stem cells. Int J Mol Sci 2022;23:11746.
22. Beken B, Serttas R, Yazicioglu M, Turkekul K, Erdogan S. Quercetin improves inflammation, oxidative stress, and impaired wound healing in atopic dermatitis model of human keratinocytes. Pediatr Allergy Immunol Pulmonol 2020;33:69-79.
23. Vinayak M, Maurya AK. Quercetin loaded nanoparticles in targeting cancer: recent development. Anticancer Agents Med Chem 2019;19:1560-76.
24. Zhao J, Liu J, Wei T, Ma X, Cheng Q, Huo S, et al. Quercetin-loaded nanomicelles to circumvent human castration-resistant prostate cancer in vitro and in vivo. Nanoscale 2016;8:5126-38.
25. Shitole AA, Sharma N, Giram P, Khandwekar A, Baruah M, Garnaik B, et al. LHRH-conjugated, PEGylated, poly-lactide-co-glycolide nanocapsules for targeted delivery of combinational chemotherapeutic drugs Docetaxel and Quercetin for prostate cancer. Mater Sci Eng C Mater Biol Appl 2020;114:111035.
26. Pons M, Foradada M, Estelrich J. Liposomes obtained by the ethanol injection method. Int J Pharm 1993;95:51-6.
27. Erdogan S, Turkekul K. Neferine inhibits proliferation and migration of human prostate cancer stem cells through p38 MAPK/JNK activation. J Food Biochem 2020;44:e13253.
28. Erdogan S, Turkekul K, Serttas R, Erdogan Z. The natural flavonoid apigenin sensitizes human CD44$^+$ prostate cancer stem cells to cisplatin therapy. Biomed Pharmacother 2017;88:210-7.
29. Ward AB, Mir H, Kapur N, Gales DN, Carriere PP, Singh S. Quercetin inhibits prostate cancer by attenuating cell survival and inhibiting anti-apoptotic pathways. World J Surg Oncol 2018;16:108.
30. Maddiboyina B, Ramaiah, Nakkala RK, Roy H. Perspectives on cutting-edge nanoparticulate drug delivery technologies based on lipids and their applications. Chem Biol Drug Des 2023;102:377-94.
31. Ayyildiz A, Koc H, Turkekul K, Erdogan S. Co-administration of apigenin with doxorubicin enhances anti-migration and antiproliferative effects via PI3K/PTEN/AKT pathway in prostate cancer cells. Exp Oncol 2021;43:125-34.
32. Munot N, Kandekar U, Giram PS, Khot K, Patil A, Cavalu S. A comparative study of quercetin-loaded nanocochleates and liposomes: formulation, characterization, assessment of degradation and in vitro anticancer potential. Pharmaceutics 2022;14:1601.
33. Quagliariello V, Iaffaioli RV, Armenia E, Clemente O, Barbarisi M, Nasti G, et al. Hyaluronic acid nanohydrogel loaded with quercetin alone or in combination to a macrolide derivative of rapamycin RAD001 (everolimus) as a new treatment for hormone-responsive human breast cancer. J Cell Physiol 2017;232:2063-74.
34. Stevens JW, Palechek PL, Griebling TL, Midura RJ, Rokhlin OW, Cohen MB. Expression of CD44 isoforms in human prostate tumor cell lines. Prostate 1996;28:153-61.
35. Read ML, Bremner KH, Oupický D, Green NK, Searle PF, Seymour LW. Vectors based on reducible polycations facilitate intracellular release of nucleic acids. J Gene Med 2003;5:232-45.
36. Constantinou C, Neophytou CM, Vraka P, Hyatt JA, Papas KA, Constantinou AI. Induction of DNA damage and caspase-independent programmed cell death by vitamin E. Nutr Cancer 2012;64:136-52.
37. Mahira S, Kommineni N, Husain GM, Khan W. Cabazitaxel and silibinin co-encapsulated cationic liposomes for CD44 targeted delivery: a new insight into nanomedicine based combinational chemotherapy for prostate cancer. Biomed Pharmacother 2019;110:803-17.
38. Hakemi P, Ghadi A, Mahjoub S, Zabihi E, Tashakkorian H. Ratio design of docetaxel/quercetin co-loading-to-nanocarrier: synthesis of PCL–PEG–PCL copolymer, study of drug release kinetic and growth inhibition of human breast cancer (MCF-7) cell line. Russ J Appl Chem 2021;94:388-401.
39. Erdogan S, Turkekul K, Dibirdik I, Doganlar O, Doganlar ZB, Bilir A, et al. Midkine downregulation increases the efficacy of quercetin on prostate cancer stem cell survival and migration through PI3K/AKT and MAPK/ERK pathway. Biomed Pharmacother 2018;107:793-805.
40. Chen C, Zhao S, Karnad A, Freeman JW. The biology and role of CD44 in cancer progression: therapeutic implications. J Hematol Oncol 2018;11:64.
41. Tsai PH, Cheng CH, Lin CY, Huang YT, Lee LT, Kandaswami

CC, et al. Dietary flavonoids luteolin and quercetin suppressed cancer stem cell properties and metastatic potential of isolated prostate cancer cells. Anticancer Res 2016;36:6367-80.
42. Hoca M, Becer E, Kabadayı H, Yücecan S, Vatansever HS. The effect of resveratrol and quercetin on epithelial-mesenchymal transition in pancreatic cancer stem cell. Nutr Cancer 2020;72:1231-42.
43. Serri C, Quagliariello V, Iaffaioli RV, Fusco S, Botti G, Mayol L, et al. Combination therapy for the treatment of pancreatic cancer through hyaluronic acid-decorated nanoparticles loaded with quercetin and gemcitabine: a preliminary in vitro study. J Cell Physiol 2019;234:4959-69.
44. Das S, Mukherjee P, Chatterjee R, Jamal Z, Chatterji U. Enhancing chemosensitivity of breast cancer stem cells by downregulating SOX2 and ABCG2 using wedelolactone-encapsulated nanoparticles. Mol Cancer Ther 2019;18:680-92.
45. Bahmad HF, Cheaito K, Chalhoub RM, Hadadeh O, Monzer A, Ballout F, et al. Sphere-formation assay: three-dimensional *in vitro* culturing of prostate cancer stem/progenitor sphere-forming cells. Front Oncol 2018;8:347.
46. Vitale D, Kumar Katakam S, Greve B, Jang B, Oh ES, Alaniz L, et al. Proteoglycans and glycosaminoglycans as regulators of cancer stem cell function and therapeutic resistance. FEBS J 2019;286:2870-82.
47. Petrova YI, Schecterson L, Gumbiner BM. Roles for E-cadherin cell surface regulation in cancer. Mol Biol Cell 2016;27:3233-44.
48. Luo G, Huang D, Tao R, Chen J. The role of *E-cadherin* - 160C/A polymorphism in breast cancer. Open Life Sci 2016;11:110-5.
49. Yu W, Yang L, Li T, Zhang Y. Cadherin signaling in cancer: its functions and role as a therapeutic target. Front Oncol 2019;9:989.
50. Martinucci B, Minatel BC, Cucielo MS, Medeiros M, Vechetti-Junior IJ, Felisbino SL, et al. Basement membrane extract attenuates the more malignant gene expression profile accentuated by fibronectin in prostate cancer cells. Mol Cell Biochem 2019;451:131-8.
51. Zhang X, Huang J, Yu C, Xiang L, Li L, Shi D, et al. Quercetin enhanced paclitaxel therapeutic effects towards PC-3 prostate cancer through ER stress induction and ROS production. Onco Targets Ther 2020;13:513-23.
52. Godwin P, Baird AM, Heavey S, Barr MP, O'Byrne KJ, Gately K. Targeting nuclear factor-kappa B to overcome resistance to chemotherapy. Front Oncol 2013;3:120.
53. Lee H, Herrmann A, Deng JH, Kujawski M, Niu G, Li Z, et al. Persistently activated Stat3 maintains constitutive NF-kappaB activity in tumors. Cancer Cell 2009;15:283-93.
54. Radhakrishnan SK, Kamalakaran S. Pro-apoptotic role of NF-kappaB: implications for cancer therapy. Biochim Biophys Acta 2006;1766:53-62.